Investigating Respiratory Rate Estimation During Paroxysmal Atrial Fibrillation Using an Improved ECG Simulation Model

Spyridon Kontaxis[1,2], Alba Martín-Yebra[1,3], Andrius Petrėnas[4,5], Vaidotas Marozas[4,5], Raquel Bailón[1,2], Pablo Laguna[1,2], and Leif Sörnmo[3]

[1]BSICoS Group, I3A, University of Zaragoza, Spain, IIS Aragón, Zaragoza, Spain
[2]CIBER de Bioingeniería, Biomateriales y Nanomedicina, Madrid, Spain
[3]Department of Biomedical Engineering, Lund University, Lund, Sweden
[4]Department of Electronics Engineering, Kaunas University of Technology, Lithuania
[5]Biomedical Engineering Institute, Kaunas University of Technology, Lithuania

Abstract

The present study addresses the problem of respiratory rate estimation from ECG-derived respiration (EDR) signals during paroxysmal atrial fibrillation (AF). Novel signal-to-noise ratios between various components of the ECG including the influence of respiration, measured by QRS ensemble variance, the amplitude of fibrillatory waves (f-waves), and the QRS amplitude are introduced to characterize EDR performance. Using an improved ECG simulation model accounting for morphological variation induced by respiration, the results show that 1. the error in estimating the respiratory rate increases as a function of the time spent in AF, 2. the leads farthest away from the atria, i.e., V_4, V_5, V_6, exhibit the best performance due to lower f-wave amplitudes, 3. lower errors in leads with similar f-wave amplitude are due to a more pronounced respiratory influence, and 4. the respiratory influence is higher in V_2, V_3, and V_4 compared to other precordial leads.

1. Introduction

Atrial fibrillation (AF) is a progressive disease, with initial episodes being self-terminating. The detection and characterization of such episodes is of paramount importance since AF burden, i.e., the percentage of time spent in AF, contributes to atrial remodeling [1]. Changes in atrial electrophysiology may be associated with alterations in respiratory physiology [2], thereby highlighting the importance of estimating respiratory parameters in AF.

Simulated ECG signals are valuable for the development and validation of diagnostic methods. A model for simulating multi-lead ECGs during paroxysmal AF (PAF) was recently proposed in the context of detection of brief AF episodes [3]. The model accounts for various morphologies of ventricular and atrial activity, AF burden, and various types of noise encountered in ambulatory recordings. In [4], an improved ECG simulation model was proposed, accounting for respiratory influence on beat morphology by rotating the vectorcardiogram (VCG) leads on a sample-to-sample basis, followed by a transformation to the standard 12-lead ECG.

In this study, the simulation model is extended by assuming that respiration not only influences the VCG leads by rotation but also by amplitude scaling. A physiological interpretation of the respiration model parameters is provided. Moreover, different signal-to-noise ratios (SNRs) are introduced to quantify the relationship between various components of the ECG including the influence of respiration, measured by QRS ensemble variance, the amplitude of fibrillatory waves (f-waves), and the QRS amplitude. Using the recently proposed slope-range technique for respiratory rate estimation [4], the performance is investigated as a function of SNR as well as AF burden.

2. Methods

2.1. Respiration signal

The dynamics of the amount of air in the lungs during the p:th respiratory cycle can be modeled as the product of two sigmoidal functions reflecting inspiration and expiration [5], see also [4, 6, 7],

$$r(n) = m_r(n) \sum_{p=1}^{\infty} \frac{1}{1+e^{\lambda_{\mathrm{I}}(p)(n-n_{\mathrm{I}}(p))}} \frac{1}{1+e^{\lambda_{\mathrm{E}}(p)(n-n_{\mathrm{E}}(p))}}. \quad (1)$$

where the steepness of the sigmoids during inspiration and expiration are defined by,

$$\lambda_{\mathrm{I}}(p) = -20\frac{F_r(p)}{F_s}, \quad (2)$$

2020 Computing in Cardiology (CinC) | 978-1-7281-7382-5/20/$31.00 ©2020IEEE | DOI: 10.22489/CINC.2020.239

$$\lambda_{\mathrm{E}}(p) = 15\frac{F_r(p)}{F_s}, \tag{3}$$

respectively, $F_r(p)$ is the respiratory rate of the p:th cycle and F_s the sampling rate of $r(n)$. The midpoint location of the sigmoids related to inspiration and expiration are defined by,

$$n_{\mathrm{I}}(p) = n_{\mathrm{O}}(p) + 0.35\frac{F_s}{F_r(p)}, \tag{4}$$

$$n_{\mathrm{E}}(p) = n_{\mathrm{O}}(p) + 0.6\frac{F_s}{F_r(p)}, \tag{5}$$

respectively, where $n_{\mathrm{O}}(p)$ is the onset of each sigmoid, defined by

$$n_{\mathrm{O}}(p) = \sum_{j=1}^{p-1} \frac{F_s}{F_r(j)}. \tag{6}$$

The function $m_r(n)$ accounts for the amplitude modulation often encountered in respiratory signals. For instance, periodic breathing can be simulated using $m_r(n) = \beta\,(1 + A_m \cos(2\pi F_m/F_s n))$, where $A_m < 1$ and F_m define the amplitude and frequency of the modulating signal, and β is a normalization factor ensuring that $r(n)$ is in the interval $[0, 1]$.

2.2. Respiratory influence on ECG

During inspiration, the heart shifts forward in a more vertical orientation due to the downward movement of the diaphragm [8]. Besides changes in the orientation of the heart vector relative to the ECG electrodes, changes in heart-to-electrode distances and impedance distribution during lung inflation cause a modulating effect on the ECG morphology [7]. This modulation has been associated with differences in stroke volume of the right and left ventricles during the different phases of respiration [9]. During inspiration, the right ventricle enlarges due to increased venous return and the pressure and volume in the left ventricle is reduced (ventricular interdependence) [10]. Thus, a decrease in ECG amplitude can be related to reduced left ventricular stroke volume during inspiration. In AF, the influence of respiration on the ventricular rhythm is negligible [11].

In this study, the simulation model proposed in [4] is extended by assuming that the VCG leads X, Y, Z are transformed not only by rotation but also by scaling on a sample-to-sample basis. The angular variation around each axis is proportional to the amount of air in the lungs. Thus, the time-varying angles $\phi_l(n)$ around each VCG lead (assuming clockwise rotation) are modeled as,

$$\phi_l(n) = \zeta_l \cdot r(n), \quad l \in \{X, Y, Z\}, \tag{7}$$

where ζ_l is the maximum angular variation. A more vertical orientation of the heart during inspiration implies a counterclockwise rotation in the planes YZ ($\zeta_{\mathrm{X}} < 0$) and XY ($\zeta_{\mathrm{Z}} < 0$), while a forward shift of the heart implies a clockwise rotation in the plane ZX ($\zeta_{\mathrm{Y}} > 0$). The amplitude scaling in each orthogonal lead is modeled as,

$$\alpha_l(n) = 1 - a_l \cdot r(n), \quad l \in \{X, Y, Z\}, \tag{8}$$

where a_l is a scaling factor. The most pronounced decrease in amplitude occurs during inspiration. The decrease in amplitude often observed in lead X may be related to the vertical orientation of the heart during inspiration [12], here modeled by $a_{\mathrm{X}} > a_{\mathrm{Z}} > a_{\mathrm{Y}}$.

2.3. Multi-lead ECG modeling during PAF

In sinus rhythm, the RR intervals are simulated using a spectral model accounting for parasympathetic stimulation and tildeoreflex regulation, whereas, in AF, the RR intervals are simulated using an atrioventricular model [3]. The switching between rhythms is modeled by a two-state continuous-time Markov chain. The time spent in each state is controlled by the AF burden parameter B ($0 < B < 1$) [3].

The ventricular activity is constructed by repeated concatenation of a single VCG QRST complex, $\mathbf{u}_{\mathrm{V}}(n)$ (3×1), until the desired length is attained. The simulated QRST complex is obtained by projecting the vector of a dipole-ECG model onto the recording leads. The resulting QRST complex is placed at the occurrence times indicated by the prevailing rhythm model, and accompanied by resampling of the QT interval according to Brazett's formula [3]. The simulated standard 12-lead ECG, $\mathbf{y}(n)$, is obtained using a linear transformation of the VCG leads [13] and adding atrial activity and noise:

$$\mathbf{y}(n) = \mathbf{D}\mathbf{A}(n)\mathbf{Q}(n)\mathbf{u}_{\mathrm{V}}(n) + \mathbf{u}_{\mathrm{A}}(n) + \mathbf{u}_{\mathrm{N}}(n), \tag{9}$$

where $\mathbf{D}$ (12×3) is the Dower matrix, and $\mathbf{Q}(n)$ (3×3) is a rotation matrix defined by the angles $\phi_l(n)$. The diagonal matrix $\mathbf{A}(n) = \mathrm{diag}\,(\alpha_{\mathrm{X}}(n), \alpha_{\mathrm{Y}}(n), \alpha_{\mathrm{Z}}(n))$ scales $\mathbf{Q}(n)\mathbf{u}_{\mathrm{V}}(n)$. The multi-lead atrial activity $\mathbf{u}_{\mathrm{A}}(n)$ (12×1) is modeled by P-waves in sinus rhythm and f-waves in AF. The noise $\mathbf{u}_{\mathrm{N}}(n)$ (12×1) is composed of baseline wander, muscle noise, and electrode movement artifacts extracted from the MIT–BIH Noise Stress Test Database [3].

2.4. ECG-derived respiratory rate

Respiratory rate is obtained from ECG-derived respiration (EDR) signals using a peaked-conditioned spectral averaging technique [4]. EDR signals are obtained using the slope range method that explores the difference between the maximum up-slope and minimum down-slope values in each QRS interval [4].

2.5. Performance evaluation

The reference respiratory rate is obtained from $r(n)$ using the spectral averaging technique applied to the EDR signals. The mean μ_{F} and standard deviation (SD) σ_{F} of the absolute error between the reference and the EDR rate are considered for performance evaluation.

To shed light on performance, the following parameters are estimated in each of the precordial leads $V_1, \ldots, V_6$: (a) the root mean square value of the noise signal $\sigma_{\mathrm{N},l}$, (b) the absolute maximum amplitude of the ensemble averaged QRS complexes $A_{\mathrm{QRS},l}$, (c) the mean of the difference between the upper and the lower envelope of the f-wave signal $A_{f,l}$, and (d) the maximum of the ensemble standard deviation of the QRS complexes $\sigma_{\mathcal{R},l}$ that reflects the influence of respiration. Then, to quantify the relationship between different components, the following SNRs are introduced:

$$\mathrm{SNR}_{\mathrm{QRS/N},l} = 20 \cdot \log_{10}\left(A_{\mathrm{QRS},l}/\sigma_{\mathrm{N},l}\right), \quad (10)$$

$$\mathrm{SNR}_{\mathrm{QRS}/f,l} = 20 \cdot \log_{10}\left(A_{\mathrm{QRS},l}/A_{f,l}\right), \quad (11)$$

$$\mathrm{SNR}_{\sigma_{\mathcal{R}}/f,l} = 20 \cdot \log_{10}\left(\sigma_{\mathcal{R},l}/A_{f,l}\right), \quad (12)$$

$$\mathrm{SNR}_{\sigma_{\mathcal{R}}/\mathrm{QRS},l} = 20 \cdot \log_{10}\left(\sigma_{\mathcal{R},l}/A_{\mathrm{QRS},l}\right). \quad (13)$$

In this study, $\mathrm{SNR}_{\mathrm{QRS/N},l}$ is set to 30 dB for all leads, while the minimum $\mathrm{SNR}_{\mathrm{QRS}/f,l}$ is set to 12 dB [4]. $\mathrm{SNR}_{\sigma_{\mathcal{R}}/f,l}$ and $\mathrm{SNR}_{\sigma_{\mathcal{R}}/\mathrm{QRS},l}$ are subject to analysis. The following parameter setup is used: $F_r(p) = 0.25$ Hz, $A_m = 0$, $F_m = 0$, $\zeta_{\mathrm{X}} = -5$, $\zeta_{\mathrm{Y}} = 5$, $\zeta_{\mathrm{Z}} = -5$, $a_{\mathrm{X}} = 0.05$, $a_{\mathrm{Y}} = 0.01$, and $a_{\mathrm{Z}} = 0.025$.

To evaluate the relationship between AF burden and performance of respiratory rate estimation for the lead closest to the atria, 50 realizations of lead V_1 are simulated for $B \in \{0.3, 0.5, 0.7\}$. For each B, the ECG is generated using the same QRST complexes and $\mathrm{SNR}_{\mathrm{QRS}/f,V_1}$ set to 12 dB. The gross median error metrics $(\tilde{\mu}_{\mathrm{F}}, \tilde{\sigma}_{\mathrm{F}})$ are computed for each B. Then, 50 different precordial leads are simulated using $B = 0.5$. For each lead, the gross median error of rate estimation $(\tilde{\mu}_{\mathrm{F}}, \tilde{\sigma}_{\mathrm{F}})$ and the gross mean and SD at different SNRs are computed.

3. Results

Fig. 1 presents the performance of respiratory rate estimation. Fig. 1(a) shows that the median errors increase as a function of B in lead V_1. Note that since the same QRST complexes were used for each B, both $\mathrm{SNR}_{\mathrm{QRS}/f,V_1}$ and $\mathrm{SNR}_{\sigma_{\mathcal{R}}/\mathrm{QRS},V_1}$ are fixed.

Fig. 1(b) shows that the best performance is obtained, as expected, in the leads farthest away from the atria. For $B = 0.5$, the largest median errors are observed in leads V_1 and V_2. Note that the error in V_1 for $B = 0.5$ is slightly higher in Fig. 1(a) since $\mathrm{SNR}_{\mathrm{QRS}/f,V_1}$ was fixed to the minimum, while in Fig. 1(b) it varies from lead to

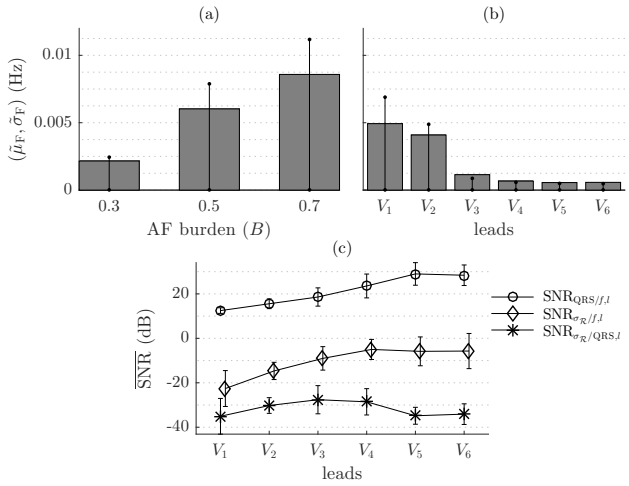

Figure 1. Performance in precordial leads. (a) The median errors in lead V_1 for different B, (b) The median errors in precordial leads with $B = 0.5$. (c) SNRs in precordial leads with $B = 0.5$. The median error metrics $\tilde{\mu}_{\mathrm{F}}$ and $\tilde{\sigma}_{\mathrm{F}}$ are denoted with tildes and lines, respectively. For each SNR, the SD is denoted with tildes around the mean values denoted with circles, diamonds, or stars.

lead. The progressive decrease in $(\tilde{\mu}_{\mathrm{F}}, \tilde{\sigma}_{\mathrm{F}})$ from V_1 to V_6 is related to the increase in $\mathrm{SNR}_{\mathrm{QRS}/f,l}$ (Fig. 1(c)). However, the changes in $(\tilde{\mu}_{\mathrm{F}}, \tilde{\sigma}_{\mathrm{F}})$ are also associated with the respiratory influences. For instance, V_3 exhibits the largest $\mathrm{SNR}_{\sigma_{\mathcal{R}}/\mathrm{QRS},l}$ (Fig. 1(c)) and thus, the most prominent decrease in the median error for adjacent leads is observed between V_2 and V_3 (Fig. 1(b)). The $\mathrm{SNR}_{\sigma_{\mathcal{R}}/\mathrm{QRS},l}$ shows a similar trend as $\mathrm{SNR}_{\mathrm{QRS}/f,l}$, however, the increment is higher in leads with more pronounced respiratory influence.

Fig. 2 illustrates respiratory rate estimation in the precordial leads with $B = 0.5$.

4. Discussion

This paper addresses the problem of respiratory rate estimation during PAF. Simulated ECGs accounting for morphological variations induced by respiration are used for performance evaluation.

The results show that the performance drops as more time is spent in AF: larger median errors are observed for higher values of B (Fig. 1(a)), resulting in a median error $(\tilde{\mu}_{\mathrm{F}}, \tilde{\sigma}_{\mathrm{F}})$ of $(0.008, 0.011)$ Hz at $B = 0.7$. In [4], where ECGs were simulated in sustained AF, the median errors were around $(0.01, 0.01)$ Hz. When the effect of AF burden on respiratory rate estimation is studied, it should also be taken into account whether AF episodes are clustered or equally distributed over time.

For $B = 0.5$, the results show that leads V_1 and V_2 are

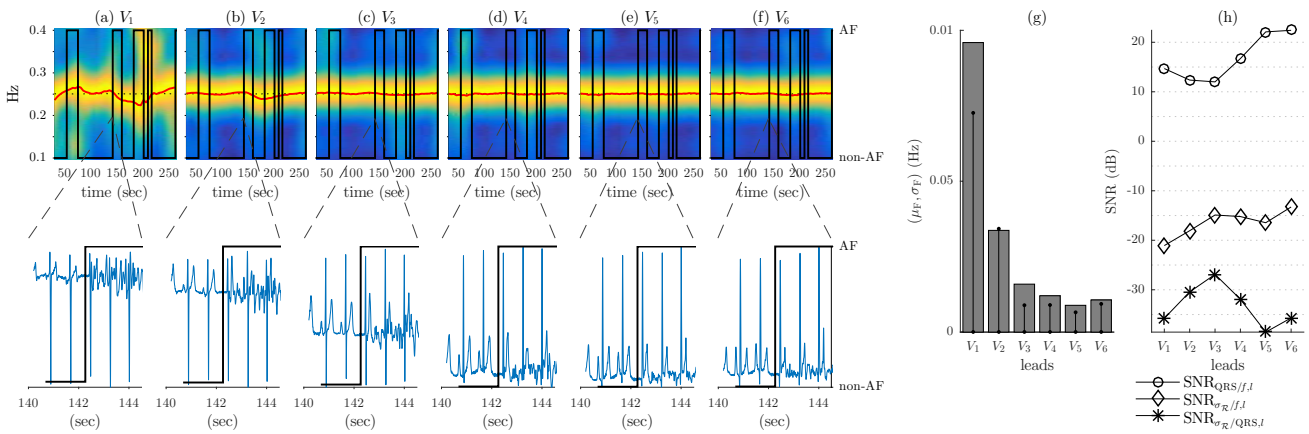

Figure 2. Example of respiratory rate estimation using $B = 0.5$. The time–frequency spectrum of the EDR signals obtained from the leads (a)–(f) V_1–V_6. The estimated respiratory rate is displayed with a red solid line, while the reference respiratory rate with a black dotted line. An excerpt of the simulated ECG signal is displayed below each time–frequency spectrum. The AF episodes (right axis) are indicated with a black solid line. (g) The error metrics μ_F and σ_F, denoted with tildes and lines, respectively, and (h) the SNRs of the simulated ECGs.

associated with larger median errors (Fig. 1(b)), mostly attributed to that the lowest $SNR_{QRS/f,l}$ is typically encountered in lead V_1. However, the respiratory influence should also be taken into account. For instance, $SNR_{\sigma_R/QRS,l}$ is higher in leads V_2, V_3 and V_4 compared to the other precordial leads (Fig. 1(c)). In Fig. 2, it can be seen that when the minimum $SNR_{QRS/f,l}$ is observed in lead V_3 (Fig. 2(h)), the estimation error is lower than that of V_1 (Fig. 2(g)) because V_3 shows larger respiratory influence indicated by $SNR_{\sigma_R/QRS,l}$. Thus, in this case, $SNR_{QRS/f,l}$ better describes the behavior of the error metrics (μ_F, σ_F).

5. Conclusions

Using simulated ECGs, the results show that the error in estimating the respiratory rate from EDR signals increases as a function of AF burden. Moreover, leads with lower f-wave amplitudes exhibit the best performance. Lower errors in leads with similar f-wave amplitude are due to a more pronounced respiratory influence.

6. Acknowledgment

This work was supported under the project RTI2018-097723-B-I00 funded by AEI and FEDER, LMP44-18 by Aragón Government (AG) and FEDER, AG with a personal grant to S. Kontaxis, European Social Fund through BSICoS group (T39_20R). The computation was performed by the ICTS "NANBIOSIS", more specifically by the High Performance Computing Unit of the CIBER in Bioengineering, Biomaterials & Nanomedicine (CIBER-BBN) at the University of Zaragoza.

References

[1] Dilaveris PE, Kennedy HL. Silent atrial fibrillation: epidemiology, diagnosis, and clinical impact. Clin Cardiol 2017;40(6):413–418.

[2] Shah V, Desai T, Agrawal A. The association between chronic obstructive pulmonary disease (COPD) and atrial fibrillation: A review. Chron Obstruct Pulmon Dis 2016;1:2.

[3] Petrėnas A, et al. Electrocardiogram modeling during paroxysmal atrial fibrillation: application to the detection of brief episodes. Physiol Meas 2017;38(11):2058.

[4] Kontaxis S, et al. ECG-derived respiratory rate in atrial fibrillation. IEEE Trans Biomed Eng 2020;67:905–914.

[5] Åström M, et al. Vectorcardiographic loop alignment and the measurement of morphologic beat-to-beat variability in noisy signals. IEEE Trans Biomed Eng 2000;47(4):497–506.

[6] Sörnmo L, et al. Databases and simulation. In Atrial Fibrillation from an Engineering Perspective. Springer, 2018; 49–71.

[7] Bailón R, Sörnmo L, Laguna P. A robust method for ECG-based estimation of the respiratory frequency during stress testing. IEEE Trans Biomed Eng 2006;53(7):1273–1285.

[8] Feher JJ. Quantitative human physiology: an introduction. Academic Press, 2012.

[9] Lamb LE. The effects of respiration on the electrocardiogram in relation to differences in right and left ventricular stroke volume: A clinical observation. Am Heart J 1957;54(3):342–351.

[10] Santamore WP, Dell'Italia LJ. Ventricular interdependence: significant left ventricular contributions to right ventricular systolic function. Prog Cardiovasc Dis 1998;40(4):289–308.

[11] Platiša, MM, et al. Uncoupling of cardiac and respiratory rhythm in atrial fibrillation. Biomed Eng 2016;61(6):657–663.

[12] Riekkinen H, Rautaharju P. Body position, electrode level, and respiration effects on the Frank lead electrocardiogram. Circulation 1976;53(1):40–45.

[13] Dower GE, et al. On deriving the electrocardiogram from vectorcardiographic leads. Clin Cardiol 1980;3(2):87–95.

Address for correspondence:

Spyridon Kontaxis (sikontax@unizar.es)
Campus Río Ebro, C/ María de Luna 1, 50018 Zaragoza, Spain